2013 IEEE/RSJ International Conference on
Intelligent Robots and Systems (IROS)
November 3-7, 2013. Tokyo, Japan

Design and Feedback Control of a Biologically-Inspired Miniature Quadruped

Onur Ozcan, Andrew T. Baisch, and Robert J. Wood
Harvard University, School of Engineering and Applied Sciences, Cambridge, MA, USA

Abstract— **Insect-scale legged robots have the potential to locomote on rough terrain, crawl through confined spaces, and scale vertical and inverted surfaces. However, small scale implies that such robots are unable to carry large payloads. Limited payload capacity forces miniature robots to utilize simple control methods that can be implemented on a simple on-board microprocessor. In this study, the design of a new version of the biologically-inspired Harvard Ambulatory MicroRobot (HAMR) is presented. In order to find the most suitable control inputs for HAMR, maneuverability experiments are conducted for several drive parameters. Ideal input candidates for orientation and lateral velocity control are identified as a result of the maneuverability experiments. Using these control inputs, two simple feedback controllers are implemented to control the orientation and the lateral velocity of the robot. The controllers are used to force the robot to track trajectories with a minimum turning radius of 55 mm and a maximum lateral to normal velocity ratio of 0.8. Due to their simplicity, the controllers presented in this work are ideal for implementation with on-board computation for future HAMR prototypes.**

I. Introduction

Due to their sizes, insects are able to locomote on smooth, uneven, vertical, and inverted surfaces with high maneuverability, agility and robustness. Even more impressively, insects do not utilize complicated control schemes to achieve such high performance locomotion. Insects utilize feed-forward, distributed controllers to control their gaits in addition to leg compliance and foot attachment mechanisms, which results in locomotion highly adaptable to different surface types [1], [2].

The locomotion capabilities of insects are the source of bio-inspiration for several terrestrial robots. These robots are able to traverse rough terrain [3], [4], access confined spaces [5], [6], and scale vertical and inverted surfaces [7], [8], [9]; hence, they are potentially useful for use in hazardous environments such as collapsed buildings and natural disaster sites. These robots are also ideal tools to investigate locomotion at small scales and to implement various mechanical designs.

From a controls perspective, there are significant differences between large and small scale legged platforms. Large legged robots such as BigDog [10], LittleDog [11], RHex [12], and AiDIN [13] have one or more degrees of freedom (DOF) per leg, which enables a varity of gaits and leg motions. On the other hand, as the robot's size decreases, the number of independent DOFs often decreases in order to avoid the size and weight of additional actuators. In addition, the payload capacity of a robot decreases significantly as it gets smaller, even though the change in payload capacity per mass is often insignificant. HAMR robots do not suffer from the former due to the design and the fabrication process used; however, they do suffer from the latter. Although most of the aforementioned small-scale robots have steering capabilities, they often operate open-loop or by remote control [4], [14]. There are a few examples of small-scale robots that employ simple controls using differential leg rotation velocity [15] or mechanical controllers such as leg compliance modulation [16] or an active tail [17]. These small-scale robots have less than one DOF per leg, and cannot adapt their gaits in order to steer the robot. There are also several small-scale robots that can alter their gaits [5], [6], [18] for steering; however, these robots do not currently employ feedback control.

This work describes the design of a new Harvard Ambulatory MicroRobot: HAMR-V shown in Fig. 1(a). This 1.07 g biologically-inspired quadruped has six actuators that enable the robot to alter its gait. Although currently without on-board electronics, the HAMR-V powertrain is optimized for payload capacity [19]; the robot can carry an additional mass of 678 mg that will be used for on-board power and control electronics in future generations. Most of this payload will be utilized by a battery, power electronics, boards, and sensors; however, a payload capacity of 50-100 mg is reserved for a microprocessor that will control locomotion. Since a processor with a mass less than 100 mg will have limited computing power (*e.g.* ATmega 168 from Atmel, mass: 60 mg, RAM: 1kB, Memory: 16 kB, Power Consumption: 27 μW), this paper also focuses on identifying the appropriate control inputs and the design of a computationally-light feedback controller for use in an autonomous version of HAMR.

II. Robot Design

Previous generations of HAMR were created to solve challenges in millimeter-scale mechanisms and actuators (HAMR2 [20]) and high voltage power electronics (HAMR3 [6]). These designs were focused on simply achieving straight, quasi-static locomotion on flat ground. HAMR2 and HAMR3 had a hexapedal design in order to maintain stability during slow speed locomotion. HAMR-V has a quadrupedal morphology inspired by dynamically-running cockroaches, which locomote quadrupedally or bipedally to reach speeds up to 1.5m/s [21]. Reducing the number of legs from six to four consequently improves manufacturability and robustness of HAMR by decreasing the number of components.

Each of HAMR-V's four legs has two orthogonal DOFs enabled by a flexure-based spherical five-bar (SFB) trans-

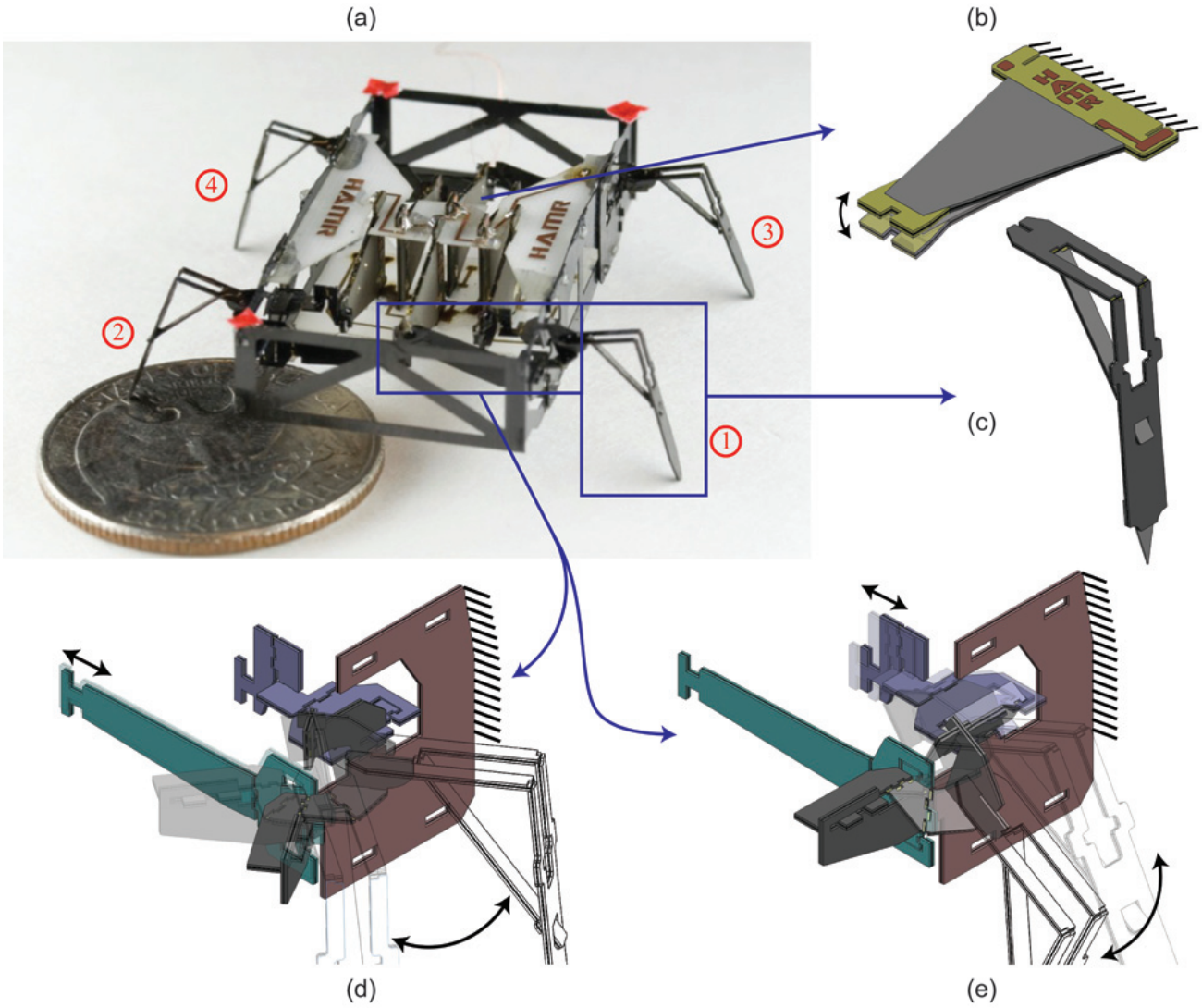

Fig. 1. (a) HAMR-V: a biologically-inspired quadruped with a mass of 1.07 g that is able to carry an additional 678 mg payload. Numbers indicate the leg naming convention. (b) Mechanical power is generated by six piezoelectric bending bimorph actuators; four control the lift DOFs and two control swing. (c) The legs are built from carbon fiber laminates, which consist of two outer carbon fiber layers and a central Kapton layer. The leg is built planar, folded to the shown geometry, and glued. (d) The transmission used to drive each leg of HAMR-V. The brown component is the mechanical ground plate. The grey components form the spherical five-bar hip joint. The light blue components form the swing DOF four-bar transmission, and the purple components form the lift DOF four-bar transmission. When the swing DOF is actuated, the actuator output is amplified through the swing DOF four-bar transmission and fed to the spehrical five-bar hip joint, which produces a rotation that swings the leg. (e) When the lift DOF is actuated, the actuator output is amplified through the lift DOF four-bar transmission and fed to the spehrical five-bar hip joint, which produces a rotation that lifts the leg.

mission previously demonstrated in [6], [19], [20]; the lift DOF raises and lowers the leg (a leg is shown in Fig. 1(c)) in the robot's sagittal plane (lift DOF actuation is shown in Fig. 1(e)), while the swing DOF provides locomotive power in the ground plane (shown in Fig. 1(d)). Each DOF of the spherical five-bar hip is driven by a piezoelectric bending bimorph actuator [22] (shown in Fig. 1(b)) through a four-bar transmission. The four SFBs and their respective four-bar transmissions are manufactured using the PC-MEMS fabrication paradigm [23], which produces meso-scale flexure-based mechanisms. The PC-MEMS components are hand assembled along with piezoelectric actuators and copper-clad FR4 circuit boards to complete the robot in Fig. 1(c).

To reduce manufacturing complexity, HAMR-V's contralateral (across-body) swing DOFs are asymmetrically coupled such that when the right front/rear leg drives rearward, the left front/rear leg drives forward and vice versa. This coupling scheme reduces four swing DOFs to two (front and rear), giving the entire robot six actuated DOFs.

Each bimorph piezoelectric actuator is voltage-driven using an alternating drive configuration consistent with [24], thus requiring a bias, ground, and signal voltage. To simplify electrical inputs, all six actuators share a single bias and single ground rail. Therefore, eight unique voltages are required for the robot: constants V_{Bias} and ground, and six drive signals, V_{s1-6}. Voltages are generated by off-

board electronics, using a controller written in Matlab and Simulink and interfaced with an xPC Target real-time testing environment. Bias and control signals are then amplified to high voltages (up to 200V) and fed to the piezoelectric actuators by 52-gauge copper wire.

The Matlab/Simulink controller can generate arbitrary input signals, therefore trapezoidal waves were chosen to drive HAMR-V's six piezoelectric actuators; a pure square wave would result in maximum ground contact per actuator cycle; however, high slew rate input signals could damage the piezoelectric ceramic. Nominally, we generate trapezoidal waves in Simulink using seven parameters: maximum voltage, minimum voltage, frequency, phase, and three duty cycles that define the rise-time, fall-time and on-time. Including the bias voltage magnitude, the total parameter space for a six DOF robot using arbitrary trapezoidal inputs is therefore 43. The explored space is reduced in this work to only parameters that will affect turning, namely by introducing an asymmetry between the robot's left and right sides. The 19 parameters used to generate walking gaits in this work are summarized in Table I and illustrated in Fig. 2. Numbered subscripts refer to each of the four legs with the following convention: 1=front left, 2=front right, 3=rear left, and 4=rear right (see Fig. 1(a)). Each parameter is listed with its nominal value for straight, quasi-static locomotion.

TABLE I

HAMR-V DRIVE PARAMETERS

Parameter	Description
$V_{\text{Bias}} = 200V$	Actuator bias voltage.
$V_{\text{L1-4}} = 100V$	Mean lift actuator drive voltage.
$V_{\text{Fr}}, V_{\text{Re}} = 100V$	Mean front (Fr) and rear (Re) swing drive voltage.
$f = 2$Hz	Gait frequency.
$\psi = 180°$	Front swing actuator phase, offset from rear swing.
$\phi_{1-4} = 90°$	Phase between lift and swing for leg i.
$D_{\text{Fr}}, D_{\text{Re}} = 50\%$	Duty cycle spent driving the leg rearward.
$D_{1-4} = 50\%$	Duty cycle spent driving leg i downward.

III. MANEUVERABILITY EXPERIMENTS

The parameters in Table I were explored to determine appropriate quasi-static turning schemes for HAMR-V. The primary goal was to achieve control of body orientation in the walking plane (θ) with the simplest possible controller (*i.e.* fewest parameters). In general, quasi-static turning is achieved by introducing asymmetry between the kinematics or frequency of left and right sides of the robot. The robot's mechanical coupling of contralateral swing DOFs precludes the use of swing mechanics to generate quasi-static asymmetry between the left and right legs. Therefore, the sagittal plane (lift) mechanics must be driven asymmetrically, contrary to the mechanics of turning in insects that primarily occurs in the walking plane [25].

Experiments were conducted on four different sets of parameters to determine their effect on robot orientation. The parameters consist of the frequency of all the drive signals, the mean drive voltage of the right and left lift actuators, the phase of the drive signal on a single leg's lift actuator, and the duty cycles of the right and left lift actuators. All experiments were conducted on flat ground using an overhead camera to track the body center of mass position (X, Y) and orientation (θ) in the walking plane. The results of these experiments are shown in Fig. 3.

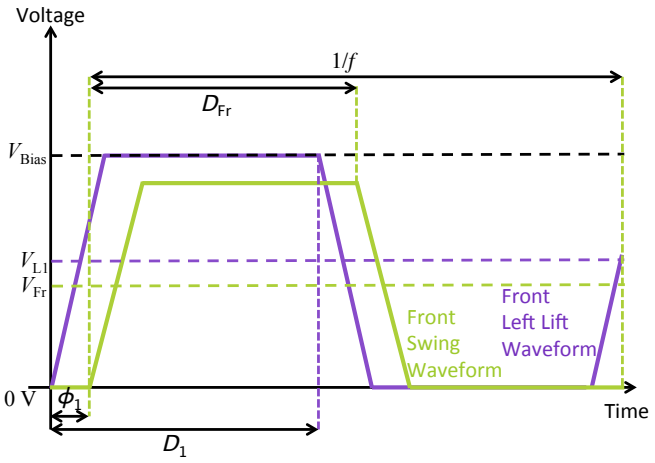

Fig. 2. Trapezoidal inputs are generated using seven values each, for a total of 43 parameters including V_{Bias}. In this work, turning strategies are employed using only 19 parameters, as listed in Table I. The red trapezoid is the drive signal for the front swing actuator and the blue trapezoid is the drive signal for the front left lift actuator.

The first set of experiments varied the frequency of each actuator drive signal, while all the other parameters were fixed at their nominal values in Table I. It should be noted that, since only one swing actuator is used for two contralateral legs, changing the stepping frequency of either side of the robot is not possible. As can be seen from Fig. 3(a), gait frequency can affect the robot's foot-ground interaction both by causing slipping and exciting dynamic modes, which lead to a change in the orientation of the robot. However, this turning method produces inconsistent results and is not considered suitable for a controller.

Additionally, the robot was tested by varying the mean lift actuator voltage V_{L1-4} on the right and left side of the body. This modification causes a change in the ground-foot interaction force on one side of the robot. The results in Fig. 3(b) show that asymmetric lift actuator voltages do have some effect on robot heading (the vector tangent to the robot trajectory at the instantaneous position) but little effect on orientation (the instantaneous angle of the robot).

A. Orientation Control

The most effective orientation control parameter for quasi-static locomotion of HAMR-V is the phase between the lift and swing DOFs (ϕ_i). Increasing/decreasing ϕ_i causes leg i to touch down later/earlier than its diagonal biped counterpart, thus rotating the robot body. Turns can be achieved by adjusting ϕ for one or more leg, however using only one leg minimizes control inputs. Figure 3(c) shows the results of tuning ϕ_1 for the front left leg, however results were similar for all four legs. By adjusting ϕ_1 to

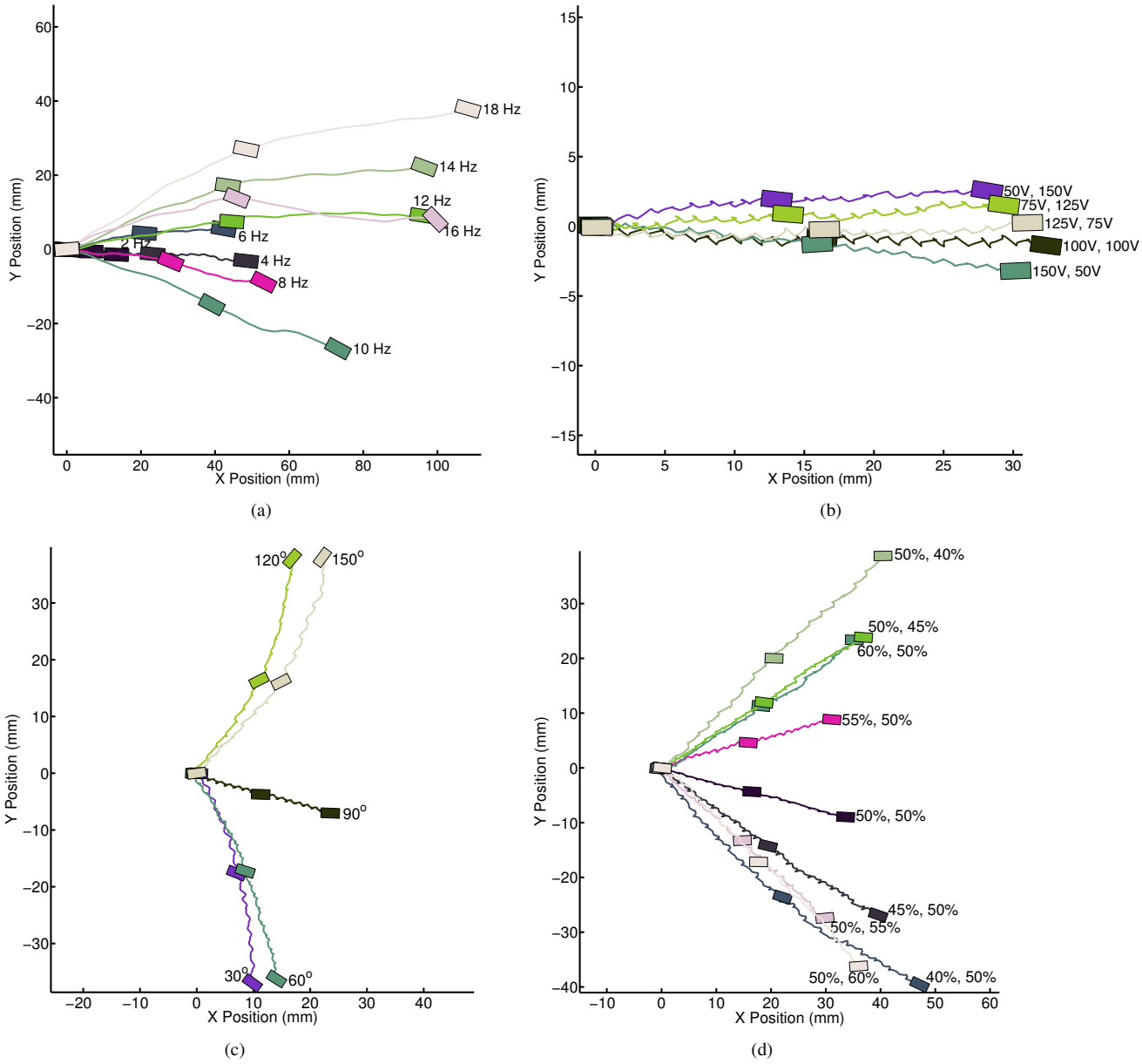

Fig. 3. Maneuverability experiments performed on HAMR-V by modifying 4 drive parameters. (a) Varying drive frequency can affect the robot's trajectory by changing foot-ground interactions. (b) Lift actuator voltage has some effect on robot heading, however does not adequately control orientation. Voltages are reported as ($V_{L1,3}$, $V_{L2,4}$) (*i.e.* (left side, right side)). (c) Varying the phase of the front left leg (ϕ_1) consistently produces left or right turns. (d) Varying the duty cycle (D_{1-4}) of the robot's lift actuators influences lateral velocity of the robot. Reported values are ($D_{1,3}$,$D_{2,4}$) (*i.e.* (left side, right side)).

be greater/less than the nominal value, left/right turns can be achieved.

B. Lateral Control

Slipping may induce lateral instabilities. Therefore, in addition to orientation control, it is desirable to find a controller that affects the lateral motion of the robot. During the feedforward maneuverability experiments, we found that varying the duty cycle of the robot's lift actuators (D_{1-4}) affected lateral velocity. Figure 3(d) shows the effect of varying lift actuator duty cycle on the robot's left or right side. It is clear from the figure that even though the robot's lateral velocity changes with different duty cycles, the orientation of the robot changes less significantly.

IV. Controller Architecture

An experimental setup was built to drive HAMR-V and implement a feedback controller. The low-level code responsible for generating the drive signal waveforms runs on an xPC target and is written in Matlab / Simulink. This code generates the analog drive signals using the digital to analog conversion board installed in the xPC target (United Electronic Industries, PD2-AO-32/16). The drive signals from the xPC target are amplified through custom high voltage amplifiers and are used to run the six actuators of HAMR-V. The host PC runs the high-level drive code and the user

interface, both written in Matlab. A camera (PixeLINK, PL-B741F) is connected to the host PC via IEEE 1394 and interfaced with the high level Matlab code. The architecture of the experimental setup is shown in Fig. 4.

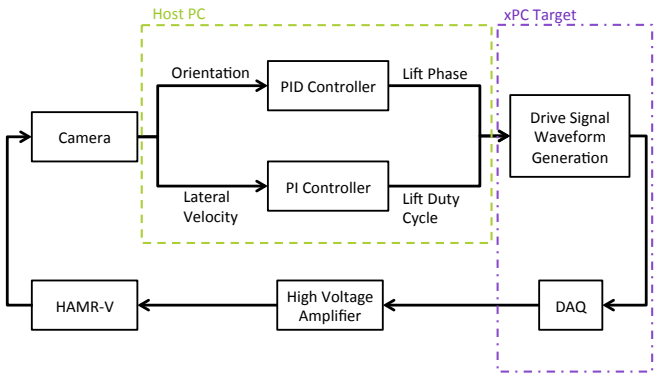

Fig. 4. The architecture of the experimental setup. The host computer collects position and orientation of the robot through a camera and runs two feedback control loops. The outputs of the control loops are sent to the drive signal generation code running on the xPC target and are fed to the robot after amplification.

The camera is used to gather position and orientation data during open-loop (operation using nominal parameters which the robot should locomote straight) and closed-loop operation. The code detects red markers on three corners of the robot frame, which are used to identify the center of mass and orientation. This center position and orientation data is then filtered using the robust local regression method (the 'rlowess' method in Matlab). After filtering the data, normal and lateral velocities with respect to the robot body are found by transforming global velocities to the robot's coordinate frame.

Maneuverability experiments show that modifying the lift phase of any leg can control robot's orientation. A PID loop is used to control the robot's orientation. This control loop takes orientation data from the camera, filters the data as described above, finds the error between the desired orientation specified by the user and the actual robot orientation, and modifies the lift phase of the front left leg. This loop runs on the host PC, and sends the new phase to the xPC target, which modifies the drive signal accordingly. The derivative of the error is found numerically using the error from current time step, the previous error and the sampling time.

We also control the lateral velocity of the robot by modifying the duty cycle of the lift actuators. A PI controller is implemented for lateral velocity control. This control loop takes the lateral velocity data, finds the error between the desired and actual speed, and modifies the lift duty cycle of the front and rear right legs. This loop also runs on the host PC and sends the modified duty cycle to the xPC target. The separation of orientation and lateral velocity controllers to different parameters on different sides of the robot enables the loops to run independent of each other.

V. Results and Discussions

Using the method described in section IV, an orientation controller (without lateral velocity control) is implemented. Due to the latency issues with Matlab's computer vision toolbox, the control loop was able to run only around 3 Hz; hence, the robot is run with 2 Hz trapezoidal drive signals.

The PID gains of the orientation controller are manually tuned: 2, 0.03, and 0.1 (proportional, integral, and derivative) are found to perform well. Desired orientations of 0, 20, and -20 degrees are used as shown in Fig. 5.

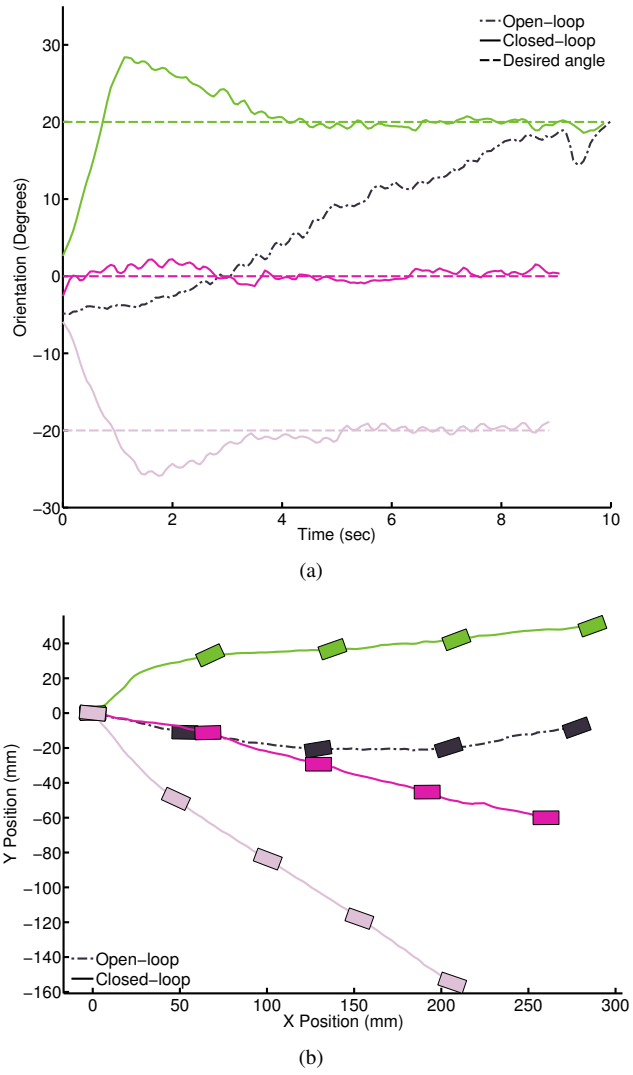

Fig. 5. The results of the orientation control experiments. (a) The dashed lines are desired orientations whereas the solid lines are actual orientation data acquired from the camera. The blue dashed-dotted line shows the open-loop trial in which the robot's orientation is not constant even with nominal drive parameters. (b) Even though the orientation of the robot is controlled, the non-zero lateral velocity of the robot prevents the controller from achieving perfect motion control.

The results in Fig. 5(a) demonstrate that the controller is able to control the robot's angle. It should be noted that small oscillations in the orientation data are caused by small changes in the observed marker positions from the stepping motion of the robot, not actual changes in the robot

angle. Although the orientation controller works properly, Fig. 5(b) shows that robot does not move along its medial axis (*i.e.* not straight forward). The robot exhibits a non-zero lateral velocity; hence the orientation controller itself is not sufficient to control robot's motion.

A lateral velocity controller is implemented and tested using a 2 Hz trapezoidal drive signal frequency. The PI gains are manually tuned to 0.1 (proportional) and 0.2 (integral). Desired lateral speeds of 10, 0 and -10 mm/sec are used. Results of these experiments are presented in Fig. 6.

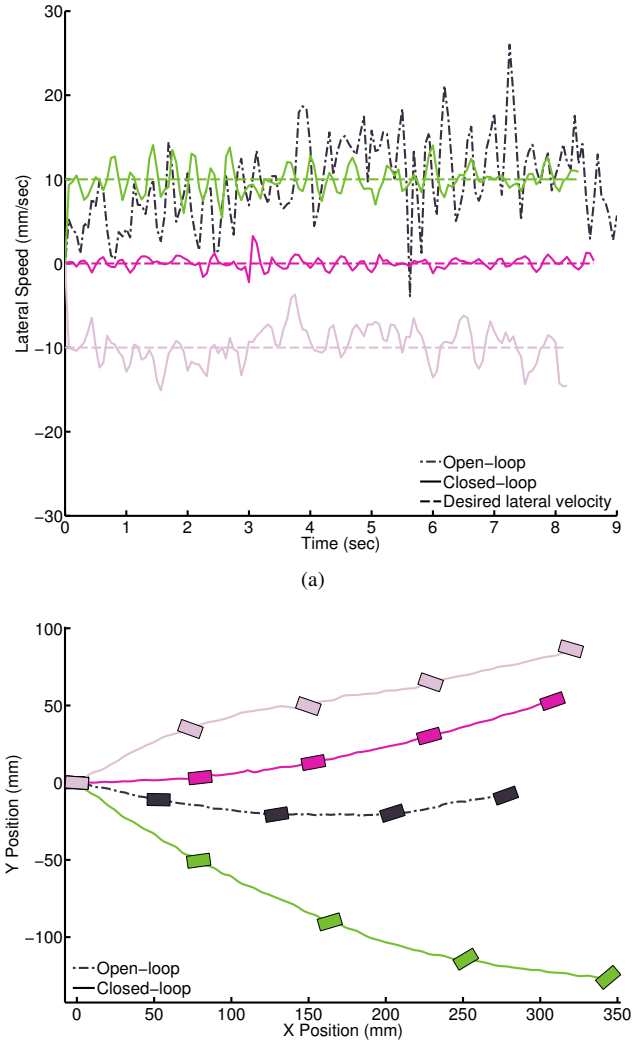

Fig. 6. Results of the lateral velocity control experiments. (a) The dashed lines are desired lateral velocities whereas the solid lines are actual lateral velocity data acquired from the camera. The blue dashed-dotted line shows the open-loop trial in which the robot's lateral velocity is increasing in time with the nominal drive parameters. (b) Similar to orientation control, the lateral controller is not sufficient to control the motion of the robot, since the robot's orientation is not constant. The noise in the lateral speed measurements are caused by tilting of the robot's body around its medial axis during stepping which is recorded by the camera.

Similar to the orientation controller experiments, the lateral velocity controller is not sufficient to control robot's motion since the orientation of the robot changes during experiments. In order to control the robot motion and follow a trajectory, the orientation and lateral velocity controllers are used together without additional modifications. Desired trajectories are generated before the control loop started. During operation, the control loop found robot position, then found the closest point on the desired trajectory and chose the desired orientation as tangent to the desired trajectory at closest point. It also chose the desired lateral velocity to be along the line connecting the robot center of mass to the nearest point on the trajectory. The results of trajectory tracking experiments are shown in Fig. 7.

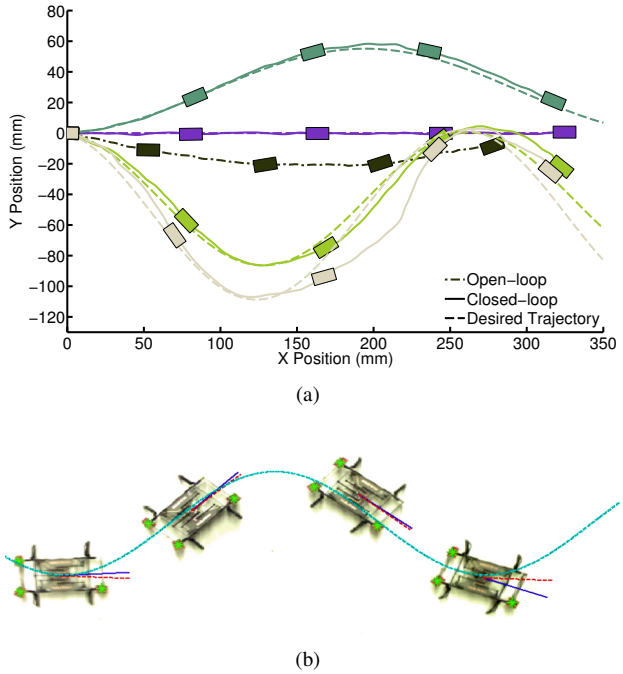

Fig. 7. The results of the trajectory control experiments in which both control loops are running. (a) The blue dashed-dotted line is the open-loop operation, the dashed lines are desired trajectories, and the solid lines are actual robot trajectories. The robot is able to follow a straight line (green line) and a sinusoidal trajectory with a radius of curvature of 150.11 mm (red curve); however, it starts to get off the trajectories as the radius of curvature decreases to 42.69 mm (light blue curve) and 33.64 mm (purple curve) which are lower than the minimum turning radius of the robot (55.40 mm). (b) Overlayed screen shots from the experiment presented with light blue in (a). The sinusoidal curve shown with light blue is the desired trajectory, the green stars are the marker locations, the red dashed line starting from the robot's center is the instantaneous desired orientation and the blue line is the robot's actual orientation. Each screen shot is two seconds apart.

The results show that while the robot does not move straight during open-loop operation, the trajectory controller can enable HAMR-V to walk straight or follow trajectories. HAMR-V has a minimum turning radius of 55.40 mm and maximum lateral to forward velocity ratio of 0.814, which are the limits of its maneuverability. The minimum turning radius and the maximum lateral to forward velocity ratio reported are obtained from the experiments in section III, and are the values obtained using only the parameters selected as the possible control parameter candidates. As shown in Fig. 7(a), the robot follows the straight and the shallow trajectory (radius of curvature = 150.11 mm) successfully, whereas its minimum turning radius does not allow the robot to perfectly

follow the trajectories with radii of 42.69 mm and 33.64 mm, shown with the purple and light blue curves. On the other hand, even though the robot cannot track the steep trajectories, it manages to gradually decrease the position and orientation error after the turns by pushing itself towards the trajectory using the lateral velocity controller.

The trajectory controller includes only two filters and two feedback control loops and all the computation is done numerically. Therefore, the trajectory controller is computationally-light (the required RAM is 44 bytes) and can be implemented on an ATmega 168 Atmel processor for example. As the next step, feedback from a nine-axis accelerometer, gyroscope, and magnetometer (MPU-9150 from Invensense) will replace the information from the camera to form the feedback loop on orientation and the lateral velocity.

VI. Conclusion

The design of the new version of HAMR, HAMR-V, is presented and its feedback control scheme is introduced. In order to achieve feedback control, an orientation controller and a lateral velocity controller are designed around the most suitable parameters found during maneuverability experiments. Trajectory following is demonstrated to prove that the controllers work properly.

This study provides valuable insights for feedback control of HAMR, proving that it is possible to control HAMR's motion using position and orientation as feedback and phase and duty cycle as control inputs. As the next step, information from a nine-axis accelerometer, gyroscope, and magnetometer (MPU-9150 from Invensense) will be used to generate on-board position and orientation feedback to improve the bandwidth of the feedback loop. Finally, on-board power and control electronics will be adopted [6] to create an untethered version of HAMR.

Acknowledgments

The authors would like to thank all Harvard Microrobotics Laboratory group members for their invaluable discussions. This work is partially funded by the Wyss Institute for Biologically Inspired Engineering and the Army Research Labs Micro Autonomous Systems and Technology Program.

References

[1] J. C. Spagna, D. I. Goldman, P.-C. Lin, D. E. Koditschek, and R. J. Full, "Distributed mechanical feedback in arthropods and robots simplifies control of rapid running on challenging terrain," *Bioinspiration & Biomimetics*, vol. 2, no. 1, p. 9, 2007.

[2] S. Sponberg and R. Full, "Neuromechanical response of musculoskeletal structures in cockroaches during rapid running on rough terrain," *Journal of Experimental Biology*, vol. 211, pp. 433 – 446, May 2008.

[3] K. Peterson and R. S. Fearing, "Experimental dynamics of wing assisted running for a bipedal ornithopter," in *Intelligent Robots and Systems (IROS), 2011 IEEE/RSJ International Conference on*, sept. 2011, pp. 5080 –5086.

[4] P. Birkmeyer, K. Peterson, and R. Fearing, "DASH: A dynamic 16g hexapedal robot," in *Intelligent Robots and Systems, 2009. IROS 2009. IEEE/RSJ International Conference on*, oct. 2009, pp. 2683 – 2689.

[5] A. Hoover, E. Steltz, and R. Fearing, "Roach: An autonomous 2.4g crawling hexapod robot," in *Intelligent Robots and Systems, 2008. IROS 2008. IEEE/RSJ International Conference on*, sept. 2008, pp. 26 – 33.

[6] A. T. Baisch, C. Heimlich, M. Karpelson, and R. J. Wood, "HAMR^3: An autonomous 1.7g ambulatory robot," in *Intelligent Robots and Systems (IROS), 2011 IEEE/RSJ International Conference on*, sept. 2011, pp. 5073 – 5079.

[7] S. Kim, A. Asbeck, M. Cutkosky, and W. Provancher, "Spinybot II: climbing hard walls with compliant microspines," in *Advanced Robotics, 2005. ICAR '05. Proceedings., 12th International Conference on*, july 2005, pp. 601 – 606.

[8] M. Murphy, C. Kute, Y. Menguc, and M. Sitti, "Waalbot II: Adhesion recovery and improved performance of a climbing robot using fibrillar adhesives," *The Internation Journal of Robotics Research*, vol. 30, no. 1, pp. 118 – 133, 2011.

[9] S. Kim, M. Spenko, S. Trujillo, D. Santos, and M. Cutkosky, "Smooth vertical surface climbing with directional adhesion," *IEEE Transactions on Robotics*, vol. 24, pp. 65 – 74, Feb. 2008.

[10] M. Raibert, K. Blankespoor, G. Nelson, R. Playter *et al.*, "Bigdog, the rough–terrain quadruped robot," in *Proceedings of the 17th World Congress*, 2008, pp. 10 823–10 825.

[11] J. R. Rebula, P. D. Neuhaus, B. V. Bonnlander, M. J. Johnson, and J. E. Pratt, "A controller for the littledog quadruped walking on rough terrain," in *Robotics and Automation, 2007 IEEE International Conference on*. IEEE, 2007, pp. 1467–1473.

[12] P.-C. Lin, H. Komsuoglu, and D. E. Koditschek, "Sensor data fusion for body state estimation in a hexapod robot with dynamical gaits," *IEEE Transactions on Robotics*, vol. 22, no. 5, pp. 932–943, October 2006.

[13] I. M. Koo, T. D. Trong, T. H. Kang, G. L. Vo, Y. K. Song, C. M. Lee, and H. R. Choi, "Control of a quadruped walking robot based on biologically inspired approach," in *Intelligent Robots and Systems, 2007. IROS 2007. IEEE/RSJ International Conference on*. IEEE, 2007, pp. 2969–2974.

[14] J. M. Morrey, B. Lambrecht, A. D. Horchler, R. E. Ritzmann, and R. D. Quinn, "Highly mobile and robust small quadruped robots," in *Intelligent Robots and Systems, 2003.(IROS 2003). Proceedings. 2003 IEEE/RSJ International Conference on*, vol. 1. IEEE, 2003, pp. 82–87.

[15] A. Pullin, N. Kohut, D. Zarrouk, and R. Fearing, "Dynamic turning of 13 cm robot comparing tail and differential drive," in *Robotics and Automation (ICRA), 2012 IEEE International Conference on*, may 2012, pp. 5086 –5093.

[16] A. Hoover, S. Burden, X.-Y. Fu, S. Sastry, and R. Fearing, "Bio-inspired design and dynamic maneuverability of a minimally actuated six-legged robot," in *Biomedical Robotics and Biomechatronics (BioRob), 2010 3rd IEEE RAS and EMBS International Conference on*, sept. 2010, pp. 869 – 876.

[17] N. Kohut, D. Haldane, D. Zarrouk, and R. Fearing, "Effect of inertial tail on yaw rate of 45 gram legged robot," in *CLAWAR, International Conference on Climbing and Walking Robots and the Support Technologies for Mobile Machines*, Baltimore, MD, USA, July 2012.

[18] J. Clark, J. Cham, S. Bailey, E. Froehlich, P. Nahata, R. Full, and M. Cutkosky, "Biomimetic design and fabrication of a hexapedal running robot," in *Robotics and Automation, 2001. Proceedings 2001 ICRA. IEEE International Conference on*, vol. 4, 2001, pp. 3643 – 3649 vol.4.

[19] O. Ozcan, A. Baisch, D. Ithier, and R. Wood, "Powertrain selection for a biologically-inspired miniature quadruped robot," in *Robotics: Science and Systems, RSS*, 2013 (Submitted).

[20] A. Baisch, P. Sreetharan, and R. Wood, "Biologically-inspired locomotion of a 2g hexapod robot," Taipei, Taiwan, 2010, pp. 5360–5365.

[21] R. Full and M. Tu, "Mechanics of a rapid running insect: two-, four- and six-legged locomotion," *Journal of Experimental Biology*, vol. 156, pp. 215–231, 1991.

[22] R. Wood, E. Steltz, and R. Fearing, "Optimal energy density piezoelectric bending actuators," *Sensors and Actuators A: Physical*, vol. 119, no. 2, pp. 476 – 488, 2005.

[23] J. Whitney, P. Sreetharan, K. Ma, and R. Wood, "Pop-up book MEMS," *Journal of Micromechanics and Microengineering*, vol. 21, no. 11, p. 115021, 2011.

[24] M. Karpelson, G. Wei, and R. Wood, "Driving high voltage piezoelectric actuators in microrobotic applications," *Sensors and Actuators A: Physical*, vol. 176, pp. 78–89, 2012.

[25] D. Jindrich and R. Full, "Many-legged maneuverability: dynamics of turning in hexapods," *Journal of experimental biology*, vol. 202, no. 12, pp. 1603–1623, 1999.